Cent. Eur. J. Geosci. • 5(1) • 2013 • 61-76
DOI: 10.2478/s13533-012-0115-x

VERSITA

Central European Journal of **Geosciences**

Long Term and Seasonal Ground Deformation Monitoring of Larissa Plain (Central Greece) by Persistent Scattering Interferometry

Research Article

Spyridoula Vassilopoulou[1]*, Vasileios Sakkas[1], Urs Wegmuller[2], Ren Capes[3]

1 National & Kapodistrian University of Athens, Faculty of Geology & Geoenvironment, Dept. of Geophysics-Geothermics, Panepistimiopolis Ilissia, 15784, Greece

2 Gamma Remote Sensing AG, Worbstrasse 225, CH-3073 Gómligen, Switzerland

3 Fugro NPA Ltd, United Kingdom

Received 20 September 2012; accepted 19 December 2012

Abstract: The land subsidence which occurs at the Larissa Basin (Thessaly Plain, Central Greece) is due to various causes including aquifer system compaction. Deformation maps of high spatial resolution deduced by the Persistent Scattering Interferometry (PSI) technique (using radar scenes from ERS and ENVISAT satellites) for the period 1992-2006 were produced to study the spatial and temporal ground deformation.
A developed GIS database (including geological, tectonic, morphological, hydrological, meteorological and water-table variation from wells in the area) offered the possibility of studying in detail the intense subsidence. The PSI based average deformation image clearly shows that subsidence generally takes place inside the Larissa Plain ranging from 5-250 mm. The largest amplitude rates (-25 mm/yr) are observed around the urban area of Larissa City (especially at Gianouli and Nikea villages), while the Larissa City center appears to be relatively stable with a tendency to subside. The rest of the plain regions seem to subside at moderate rates (about 5-10 mm/yr). The surrounding mountainous area is stable, or has slightly been uplifted with respect to the NE located reference point. It was found that there is a correlation between the seasonal water-table variation (deduced from wells data), the seasonal water demand for irrigation associated with specific types of cultivation (cotton fields), the monthly rainfall, and the observed subsidence rate in the rural regions of the Thessaly Plain.

Keywords: Ground Deformation • Persistent Scattering Interferometry • Terrain Analysis • GIS.Larissa (Greece)

1. Introduction

Larissa is located at the Eastern Thessaly Plain. Thessaly's total area is about 14.036 km^2. The Pinios River and its tributaries drain the entire hydrologic basin of Thessaly. It is surrounded by mountainous areas which form its watershed [1]. The Titaros Mt. (1.837 m) and the Kamvounia Mt. (1.615 m) lie to the north, to the northeast are the Olympos Mt. (2.917 m) and the Ossa Mt. (1.978 m), to the east is the Pilio Mt. (1.548 m), to the south is the Orthrys Mt. (1.726 m), to the west are the Pindos Mt. (2.204 m) and the Koziakas Mt. (1.901 m).

*E-mail: vassilopoulou@geol.uoa.gr

Internally, the plain is divided by a low-lying hill area into a western part (Trikala-Karditsa) and an eastern part (Larissa) [1]. Summers in Thessaly are usually very hot and dry. Mean annual precipitation over the area is about 700 mm and it is distributed unevenly in space and time. The mean annual precipitation varies from about 400 mm at the Palin area to more than 1850 mm at the western mountain area [2]. Rainfall is rare from June to August.

The Thessaly Plain is the most productive agricultural region of Greece. The main crops cultivated in the plain area are cotton, wheat and maize, while apple, apricot, cherry, olive trees and grapes are cultivated at the foothills of the eastern mountains. The intense and extensive cultivation has led to the highest water demand in Greece for agricultural use, which is usually fulfilled by the over-exploitation of ground-water resources. Although Pinios River is the third longest river in Greece, only a small part of this demand is covered by the Pinios River, its tributaries, as well as a few small reservoirs and lagoons adjacent of Pinios River [3]. Even though a small part of the population in Greece (about 1%) lives in the Thessaly Area, the water consumption is 18.5% of the total water consumption in Greece, while 95% of the water consumption is for agricultural use [4].

The increased water demand has been associated with severe extreme and persistent drought episodes in the last decades [2, 5]. The dry conditions resulted in irrigation cutbacks, over-exploitation of ground-water and significant losses of crop fields. The increased water demand resulted in the drilling of a significant number of wells in the Thessaly plain, as well as in the broader area of Larissa.

Land subsidence due to large amounts of water withdrawal from an aquifer has occurred in numerous regions throughout the world and is characterized as a potential risk for subsidence especially in cases where the overlapping surface is a built up area [6, 7].

The magnitude and areal extent of such deformation is not easily detectable with classical geological and geotechnical methods, which are normally expensive and time-consuming. A great number of researchers demonstrated the capability of differential InSAR to detect and measure ground subsidence, caused by the removal of subsurface groundwater, which in the case of the Persistent Scatterers Interferometric (PSI) technique is of millimeter-scale, i.e. [8–10].

ERS and ENVISAT satellite radar images (1992-2006) for the Thessaly Plain were processed by GAMMA software and ground displacement measurements were produced by PSI technique within this study.

Deformation data deduced by PSI processing were combined with all the available information (geology, tectonic, morphology, hydrogeology and water-table variation from the wells in the area, meteorological data) in a GIS data base, in order to create thematic and synthetic maps as well as diagrams for the land subsidence monitoring. Meteorological and Hydrogeological data together with water-table variation from water-wells in the area covering the observational period 1992-2006 were taken into consideration in this study.

2. Geological and Tectonic Setting

Larissa Basin is a tectonically active region [11–13]. Several moderate magnitude earthquakes (M>5) have occurred in the last century. Some of these earthquakes caused damage to a large number of areas while two of them were associated with the reactivation of major Quaternary normal faults and surface ruptures [14–17].

On June 9, 2003 Northern Thessaly was shaken by a moderate magnitude earthquake (MS=5.5; NOA). Dozens of buildings in the area of southern (or lower) Mt Olympus were damaged [18].

The present-day morphology of Thessaly is basically associated with the Neogene tectonic phase caused by the post-orogenic collapse of the External Hellenides [11]. The NE-SW extension (Late Miocene-Early Pleistocene) generated a series of horsts and grabens bordered by NW-SE trending faults (Fig. 1). The main NW-SE trending basins of Karditsa and Larissa were produced by NW-SE trending normal faults [11].

After a period of quiescence, a new roughly N-S extension affected the Aegean Region. A new system of normal faults was generated mainly trending E-W to ESE-WNW (Fig. 1), according to Caputo et al (1990) [19]. This deformational phase started during the Middle to Late Pleistocene and is still active as can be deduced by the recent seismicity of the area, e.g. [14, 15]. The majority of these faults form grabens, which cross-cut the older structures and uplift and offset Late Quaternary deposits. The Tyrnavos Fault is one of the major active structures bordering the homonymous basin [19–21].

The geological structure is given in the simplified geological map (Fig. 2), according to Athanassiou (2002) [22]. The plain is covered by a thick (up to 50 m deep) alluvium layer, which is of a Quaternary Lake, which was gradually restricted to the Karla Lake in the SE part. Karla Lake was artificially drained in the 1960s to provide cultivated land [23]. The Quaternary deposits can be distinguished as: Alluvial sediments that cover the Plain of Larissa, Fluvial terraces (Penios river) and Lacustrine deposits. Some Pleistocene fissure fillings occur in

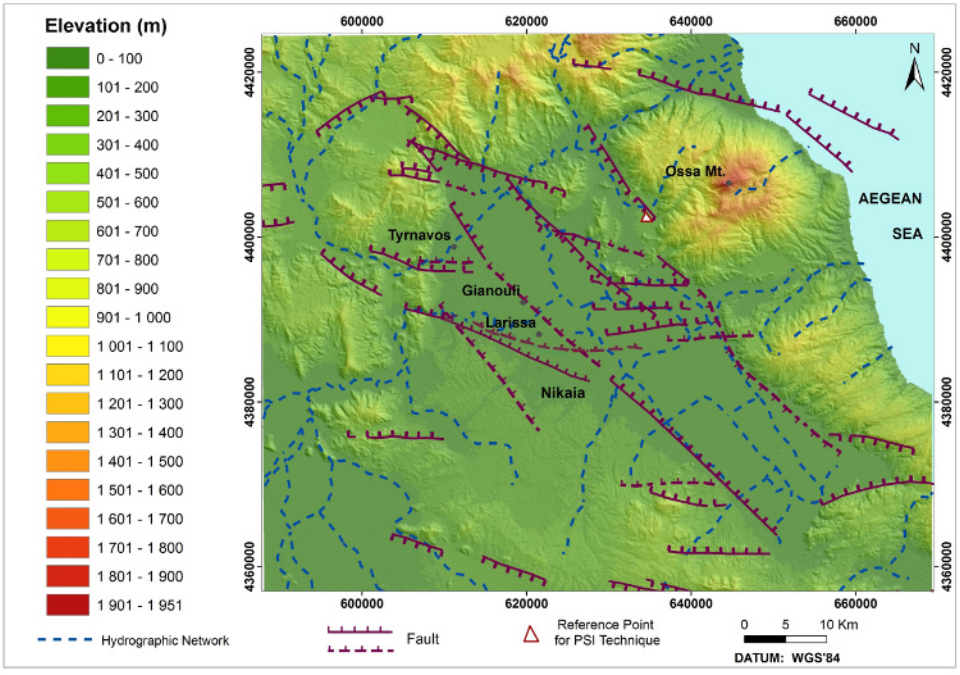

Figure 1. The shaded relief of the study area based on the 25 metre resolution ASTER GDEM (a product of METI and NASA) with the faulting zones according to Caputo (1990) & Caputo et al (1993). The terrain is rough and depends on tectonics, mainly.

the karstic limestones and marbles of the basement. The Alpine formations include Late Cretaceous-Eocene Flysch, Neritic Mesozoic Limestones, Marbles and Dolomites (Late Mesozoic-Palaeocene), Phyllite, Schists with marbles intercallations, Schist-Chert Formations of Jurassic age, Gneisses, Schists and Amphibolites of Palaeozoic-Triassic age and Ophilolites. The Alpine basement that occurs in the Central-Eastern Thessaly Plain belongs to the Pelagonian, Sub-Pelagonian, and Olympus-Ossa Geotectonic Units [24].

3. The Subsidence in the Larissa Plain

During the study of the hydrogeological conditions in the broader area of Larissa from the Greek Institute of Geology and Mineral Exploration [25], strong land subsidence was observed which was caused by the rapid groundwater over-pumping. The occurrence of the land subsidence and its associated effects during the last years at the Larissa Basin mobilized the local and governmental authorities.

Three types of ground deformation have been reported in the Thessaly Plain since 1986, including ground fissures, sinkholes and land subsidence [23]. Numerous fissures opened up across the Thessaly Plain mainly at its eastern part, affecting cultivated land, roads, houses and even the area of the NATO Larissa airport. Most of these fissures had an opening of up to several tens of centimetres, presenting also an expansion rate of up to 30 mm/year. The maximum amplitude of opening took place between August and October, when the ground water pumping was at a maximum and the water table level at a minimum. The observed ground fissures in Thessaly Plain do not represent precursors of oncoming earthquakes and they clearly do not originate from earthquake-related effects; they are simply caused by sediment compaction resulting from rapid groundwater level decline following intensive, uncontrolled water pumping [23].

Several small-diameter (about 20 cm) sinkholes have also been observed mainly close to irrigation wells. Land subsidence has been reported by Kaplanidis and Fountoulis (1997) [26] from evidence in well casings. However, there was no sign of ground fissures or damages to buildings and roads, indicating a rather uniform subsidence or subsidence with a small gradient deformation.

The mapped important E-W component of ground motion after DInSAR analysis is due to tectonic processes while

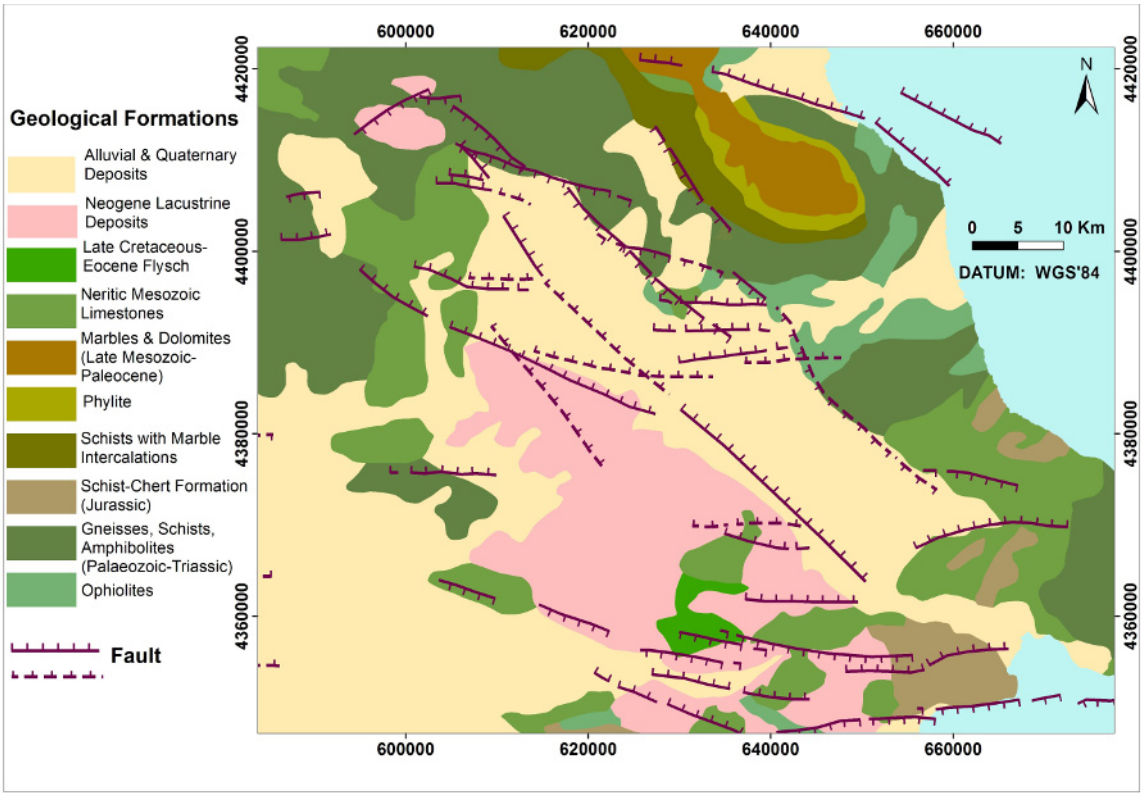

Figure 2. The geological structure of the broader area of Larissa Plain is given according to Athanassiou (2002). Alluvial and Quaternary deposits, Post-Alpine and Alpine formations cover the study area. The thematic layer was produced using ArcGIS 9.3 & 10 and is included together with other thematic and synthetic data and diagrams in the database corresponding to their correlation and analysis.

the data for the Larissa City show clear subsiding trend with periodic behavior which is related to the hydraulics of the aquifer, while the fluctuations become clearer after 1996 [27–29].

It is noted that the land subsidence due to sediment compaction following fluid withdrawal is a phenomenon which is observed in various areas of the world and has been studied extensively [30–33].

4. Methodology and Data

4.1. The PSI InSAR Technique

Deformation maps of the broader area of Larissa were deduced by the PSI InSAR technique using ERS and ENVISAT satellite radar images, ranging from November 1992 to February 2006. The date of the reference satellite image for the analysis of the ground deformation was the February 23, 1997 (Table 1), while the reference point for the ground deformation study was set at the mountainous area NE of the Larissa City (Fig. 1).

4.2. Introduction to the Interferometric Point Target Analysis

Interferometric Point Target Analysis (IPTA) is a method used to exploit the temporal and spatial characteristics of interferometric signatures collected from point targets to accurately map surface deformation histories, terrain heights, and relative atmospheric path delays. The use of targets with point like scatter characteristics has the advantage that there is much less geometric decorrelation. This permits phase interpretation even for large baselines above the critical one. Consequently, more image pairs may be included in the analysis. Important advantages of the technique are the potential to find scatterers in low-coherence areas and that interferometric image pairs with large baselines may be included in the analysis. Finding usable points in low-coherence regions fills spatial gaps in the deformation maps while the ability

Table 1. Dates of Radar Images used in the Larissa Terrafirma Product.

Date	Julian Day	Days
12/11/1992	2448939	-1564
10/06/1993	2449149	-1354
25/03/1995	2449802	-701
29/04/1995	2449837	-666
30/12/1995	2450082	-421
31/12/1995	2450083	-420
09/03/1996	2450152	-351
13/04/1996	2450187	-316
14/04/1996	2450188	-315
18/05/1996	2450222	-281
19/05/1996	2450223	-280
19/01/1997	2450468	-35
23/02/1997	2450503	0(*)
04/05/1997	2450573	70
24/05/1998	2450958	455
28/06/1998	2450993	490
28/02/1999	2451238	735
13/06/1999	2451343	840
05/12/1999	2451518	1015
23/04/2000	2451658	1155
28/05/2000	2451693	1190
24/12/2000	2451903	1400
13/01/2002	2452288	1785
02/06/2002	2452428	1925
24/11/2002	2452603	2100
09/03/2003	2452708	2205
28/03/2004	2453093	2590
02/01/2005	2453373	2870
06/02/2005	2453408	2905
13/03/2005	2453443	2940
17/04/2005	2453478	2975
17/04/2005	2453478	2975
22/05/2005	2453513	3010
22/05/2005	2453513	3010
13/11/2005	2453688	3185
22/02/2006	2453793	3290

(*)The date of the radar image used as reference for the PSI analysis

to use large baselines improves the temporal sampling. A more detailed discussion of the point target based interferometric technique is provided by Wegmüller *et al.* (2004) [34].

The most straightforward application of IPTA is the monitoring of slow and temporally uniform deformation. In this case the temporal and spatial sampling of the signal is very good. In the case of high deformation rates, the capability of the point target based interferometric technique to use pairs with large baselines has the advantages that high phase gradients can be reduced if shorter observation intervals become available. In addition, large scale corrections such as baseline errors and the large scale component of the atmospheric distortions can be estimated independently of the areas with high deformation gradients and interpolated or extrapolated to get relatively accurate corrections for the entire area. The spatial separation of the available point-like scatterers is an important factor. Larger distances (lower spatial sampling) strongly reduce the potential to resolve high phase gradients. In the case of temporally strongly varying deformation rates, spatial unwrapping of the point phases is necessary.

4.3. Radar Data

While archived data are excellent for the assessment of deformation histories, near real-time monitoring depends on new acquisitions. ENVISAT was operated in the same tracks as the ERS satellites, although at a slightly different carrier frequency, which has a strong influence on across-sensor interferometry. An approach was developed for the integration of ERS and ASAR data into the Interferometric Point Target Analysis [35]. An important advantage of the use of targets with point like scatter characteristics in a SAR interferometric analysis is that coherence is maintained for many scatterers across series including both ERS and ENVISAT data, in spite of the slightly different sensor carrier frequencies. An integration of ERS - ASAR series is very relevant for time monitoring. Furthermore, the accuracy of time monitoring based on a smaller number of ASAR acquisitions can be improved through the integration of additional ERS acquisitions, such as through a better identification of adequate points and through a more accurate estimation of the related point heights. For the Larissa data IPTA processing, a total of 74 scenes (62 ERS and 12 ASAR scenes) were considered in the analysis.

The Larissa data processing was exceptionally challenging for three main reasons. The first reason was that relatively small to medium scale atmospheric distortions were presented in many scenes (this means about 1 km to 20 km horizontal range), especially during summer time. The second reason was the presence of very strong, i.e. up to 5 cm and more, small to medium scale seasonal deformation effects. Furthermore, the spatial coverage of the interferometric information has significant spatial gaps in the agricultural areas around Larissa.

After extensive tests and processing trials, it was decided to base the analysis on the winter/spring data acquired between December and June, only. The reason was the problems with the phase unwrapping for data acquired in summer/fall. These problems are caused by poorly

sampled but significant phase gradients caused by a combination of the reasons mentioned in the previous paragraph. For the selected winter/spring times the subsidence was found to be sufficiently uniform in time, excluding the seasonal effects and the strongest atmospheric distortions, so that the phase unwrapping could be reliably resolved. There remains some uncertainty for the smaller and more isolated settlements mainly to the East of Larissa.

The main results of the IPTA processing were the linear component of the deformation rate. The approach used included SLC co-registration to common SAR geometry (taking into account terrain height effects), point list determination from SLC spectral and radiometric characteristics, initial point height estimation using SRTM 3" DEM based heights, refinement of initial baselines from orbit data based on point differential interferograms and height control points derived from reference DEM. The main results of the IPTA analysis consist of refined baselines, improved point heights, linear deformation rates, atmospheric phase corrections, residual phases, quality information, and the point wise time series for the selected winter/spring dates. For further use the results were terrain corrected geocoded, considering point heights, and visualized.

Two characteristic differential interferograms in Fig. 3 show the strong seasonal effects and the atmospheric effects.

5. GIS Database Management for the broader Area of Thessaly Plain

A large number of various data from different sources, in different format, scale and map projections had to be compiled. The collected information (deformation data deduced by PSI technique, topographical, geological, tectonic, meteorological and hydrological data) was organized in a GIS database using ArcGIS v. 9 & 10 software. Thematic and synthetic layers in vector format were compiled in a common cartographic system in order to produce maps and diagrams. The database management provided information about the main characteristics of the tectonic, morphotectonic, ground deformation and other features (eg. main fault directions, places of strong ground deformation). Ground deformation interpretation was based on the interpretation of all the thematic layers and maps as well as on the various diagrams which were created.

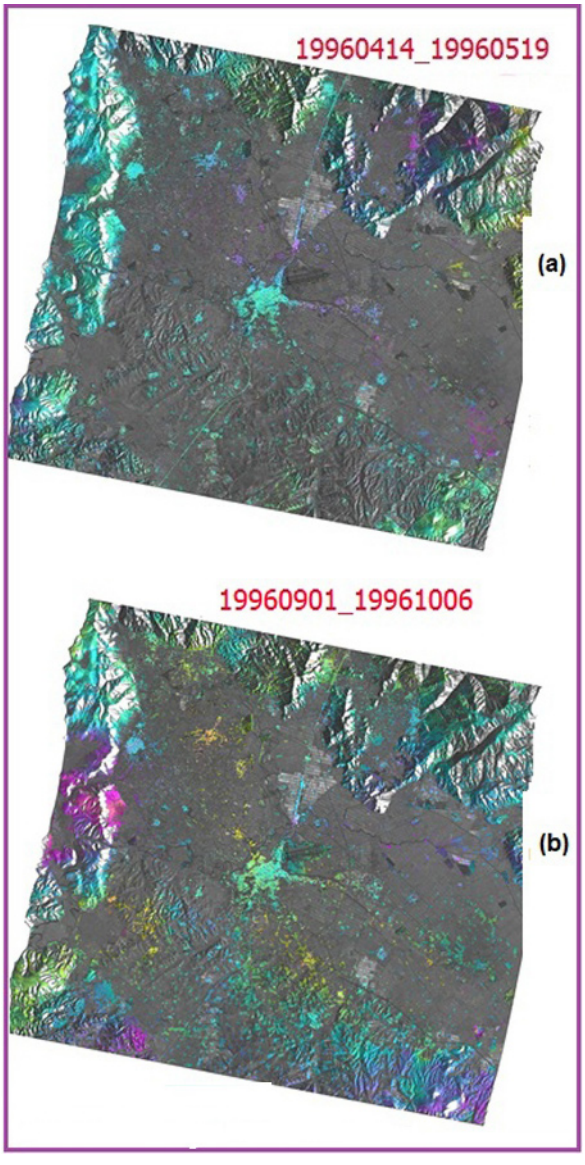

Figure 3. Two differential interferograms are given where the strong seasonal effects as well as the atmospheric effects are apparent. a) The subsidence for Larissa Plain and Nikea Village is evident in the first interferogram (19960414_19960519). The Atmosphere is characterised as moderate to strong. b) The uplift for Larissa Plain and subsidence for Nikea Village are observed in the second interferogram (19960901_19961006), where the atmosphere is strong.

A. Geological and Terrain Analysis Data

The Tectonic and Geological map of the area (Fig. 1 & Fig. 2, respectively) together with terrain analysis layers were created aiming to facilitate the interpretation of the PSI image. A Digital Elevation Model with a resolution of 25 meters (Fig. 1) was produced using the ASTER

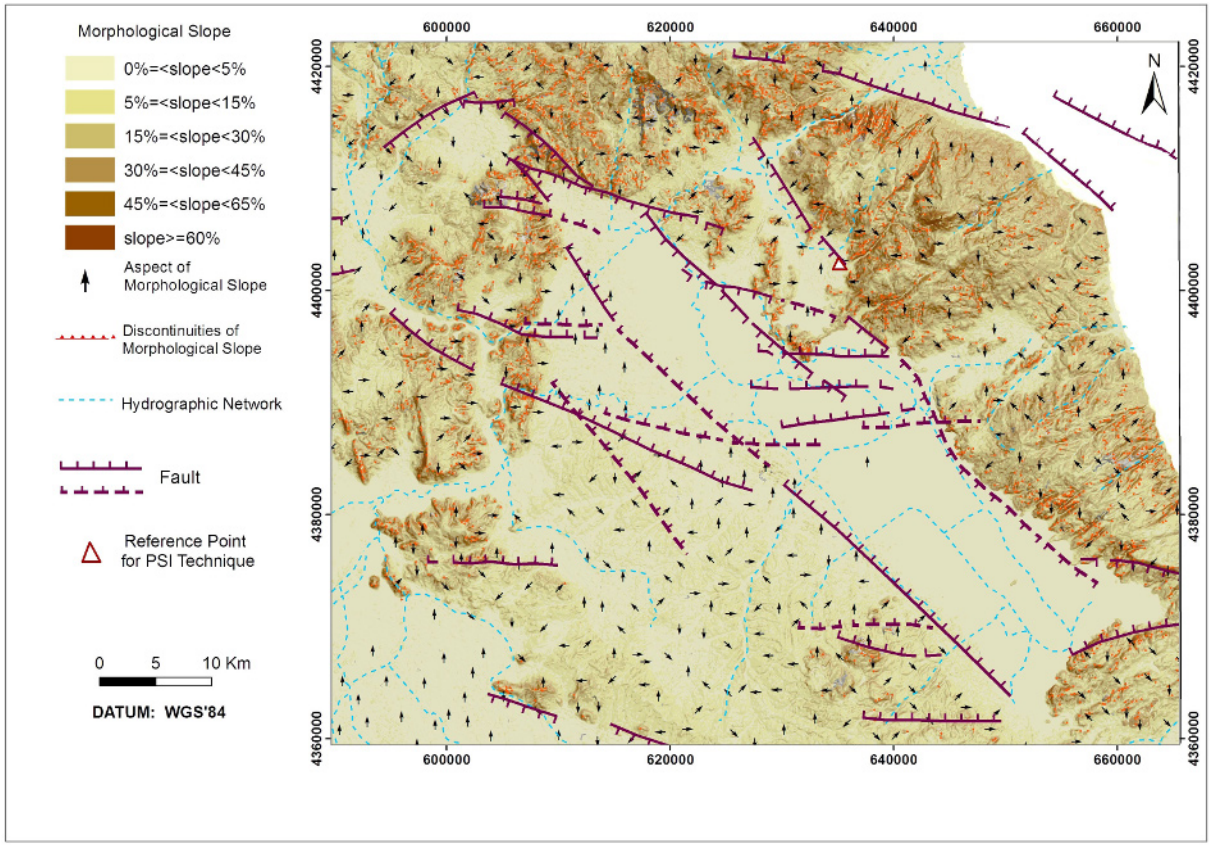

Figure 4. Intense morphological slopes with morphological discontinuities around Larissa Plain can be distinguished after the terrain analysis using the software PROANA-II. These data will be used for the statistical analysis in relation to the tectonic data (Fig. 5).

GDEM data of the area (a product of METI and NASA) and was used for the terrain analysis data creation. The following maps were made using the "PROANA-II" software (updated version of the "PROANA" [36, 37]):

"Map of Morphological Slopes" which represents the slopes of the terrain classified in regions (0-5%, 5-15%, 15-30%, 30-45%, 45-60%, slopes >60%) as well as the aspect of the slopes (the angles are categorized by 45°).

"Map of Discontinuities of Morphological Slopes" which represents the differences in slope more than 10%.

"Map of Drainage Network"

"Terrain Analysis Map" (synthetic map which includes all the features for terrain analysis, Fig. 4)

"Shaded Relief" as well as draping thematic maps (geological, tectonic etc) over the DEM produce more realistic images for the analysis and interpretation.

Also, diagrams were produced after statistical analysis of terrain data including rose diagrams of faults (Fig. 5a), a rose diagram that represents the terrain orientation (Fig. 5b) and rose diagrams of morphological discontinuities (Fig. 5c).

B. Ground Deformation Data

The deformation data, based on the PSI analysis, were also included in the GIS database of the area and the following maps and diagrams were created: A high spatial resolution "Deformation Map" (Fig. 6) was created for the broader area of Larissa Plain during 1992 to 2006. The ground deformation velocity (mm/year) was divided into six (6) classes after statistical analysis (-32 to -15 mm/year, -15 to -10 mm/year, -10 to -5 mm/year, -5 to -2 mm/year, -2 to 0 mm/year, 0 to 2 mm/year). The deformation velocity of the vertical motion was studied along characteristic profiles (Fig. 7, Fig. 8). The vertical motion for some selective points (Fig. 7), deduced from the PSI processing, in relation to the time, can be represented

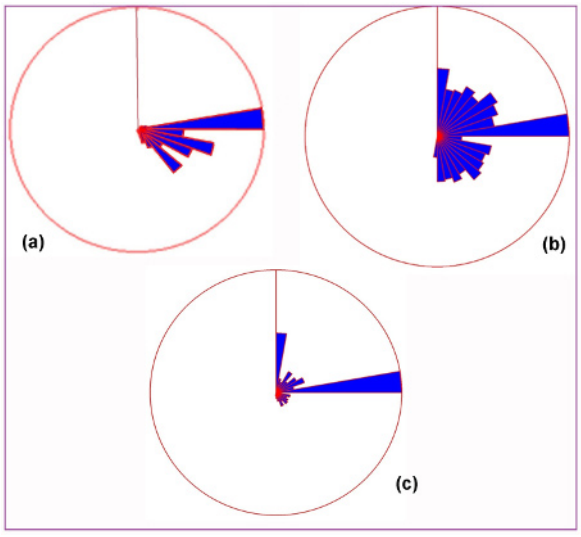

Figure 5. a) A main E-W direction as well as the ESE-WNW and SE-NW directions of the faulting zones can be observed in the rose-diagram. b) The main terrain direction is the E-W but other directions can also be observed. c) The main direction of the discontinuities of morphological slopes is the E-W. The N-S and other directions can be observed too.

on a diagram automatically, using PROANA-II software (Fig. 9). These diagrams represent the "Time Series of the Deformation" of each selective point.

C. Meteorological and Hydrogeological Data

Maps based on the hydrogeological data and various diagrams such as: the rainfall for the last years and the seasonal water table variations showing the systematic drop of the water table etc., were produced using the meteorological and hydrogeological data, and will be presented in the following paragraphs.

6. Terrain Analysis

Interesting results about the tectonics and morphotectonic characteristics of an area can be derived studying the terrain in detail. DEM is the basic feature in the terrain analysis of a region, since it can be used as a base for thematic applications (e.g. geology, volcanology, geophysics, orthorectified satellite images, interferometry), and as a base for production of a great variety of maps relating to the terrain analysis. The DEM of the broader area of Larissa was used as base map, and for the production of the terrain analysis data.

Based on the geological, tectonic and terrain analysis data it is evident that Larissa Basin represents a surface planation (typical plain), which is traversed by the Pinios River. It has a NW-SE direction and extends from the northern to the southern part of the study area, in the central part, while NW-SE faulting zones are the borders of the basin (Fig. 1). Around the basin and especially at the eastern and northern part, where high mountains surround the plain, the terrain is characterized as rough. Intense morphological slopes with morphological discontinuities of the slopes have been distinguished after terrain analysis (Fig. 4). The elevation ranges from sea level at the eastern coastal area to more than 1900 m at the eastern and western mountain areas, and the mean elevation of the region is nearly 270 m (Fig. 1). The mean elevation of the Larissa Basin is about 70 m (Fig. 1).

For the calculation of the principal directions of the linear features (tectonic and morphological) the ArcGIS software/Rose Diagram ArcScript was used. A main E-W direction as well as the ESE-WNW and SE-NW directions of the faults can be observed in the rose-diagram (Fig. 5a). The main terrain direction is the E-W (similar to the main direction of the faults) but the N-S, NE-SW and SE-NW directions can be observed in the rose diagram too (Fig. 5b). The main direction of the discontinuities of morphological slopes is also E-W (Fig. 5c) while N-S and other directions can be observed. There is a correlation between the directions of the tectonic data and the terrain. It is noted that the all the data were processed and the lengths of them have been involved for the direction calculation.

7. Ground Deformation Analysis

Comparing the PSI deformation data with the geological, and terrain data, it is observed that the higher rates of ground subsidence have been measured on the alluvial formations in the Larissa Basin, while small or insignificant land subsidence has occurred on the Alpine formations around the mountainous area.

Analytically, the combination of the PSI deformation data with the geological, tectonic, morphological and hydro-geological data provides the following results:

The largest amplitude rates (-25 mm/year) are basically measured around the urban area of Larissa City, especially at Gianouli and Nikea Villages, along the NW-SE faulting zone which passes through (Fig. 1, Fig. 6, Fig. 10) while the Larissa City appears to be relatively stable with a tendency to subside. NW-SE and E-W faults are the boundaries of the region (Fig. 10), while thick Alluvial and Quaternary Deposits cover Tyrnavos-

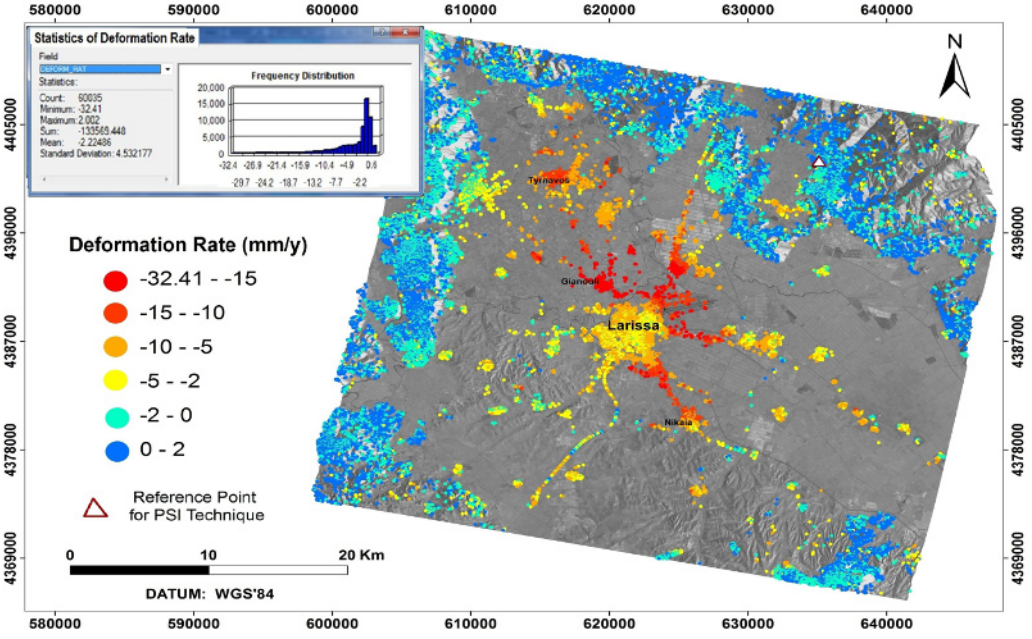

Figure 6. Deformation map of the broader area of Larissa Plain based on the PSI InSAR technique using ERS and ENVISAT satellite radar images ranging from November 1992 to February 2006. The classification of the deformation rate in categories was given according to statistical analysis of the deformation rate.

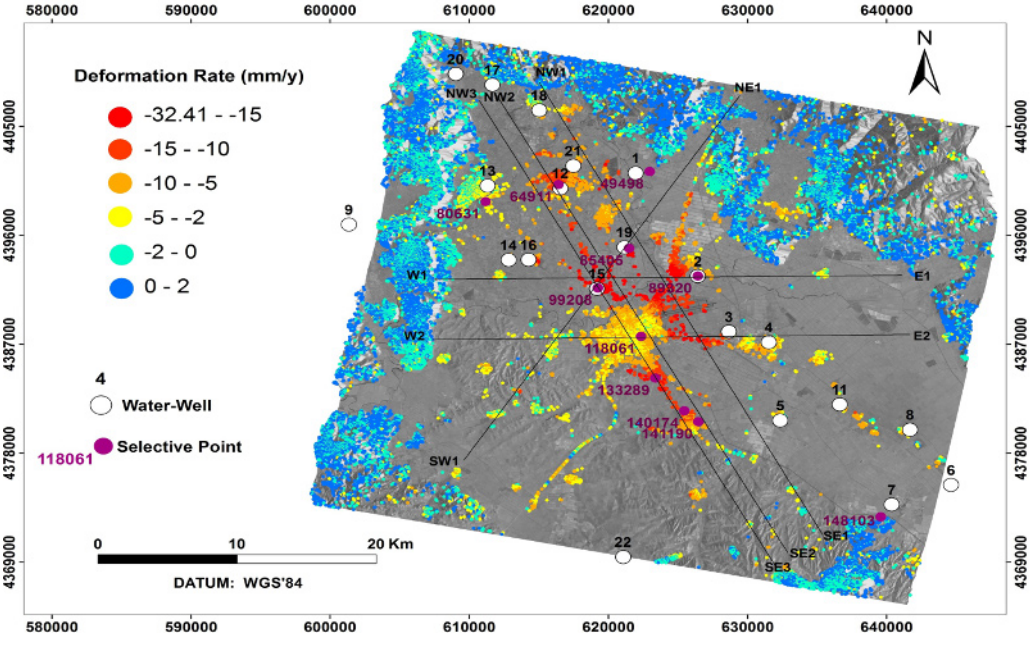

Figure 7. The deformation rate was studied along six characteristic profiles: W1-E1, W2-E2, NW1-SE1, NW2-SE2, NW3-SE3, NE1-SW1. The locations of the selective points and water-wells are also noted.

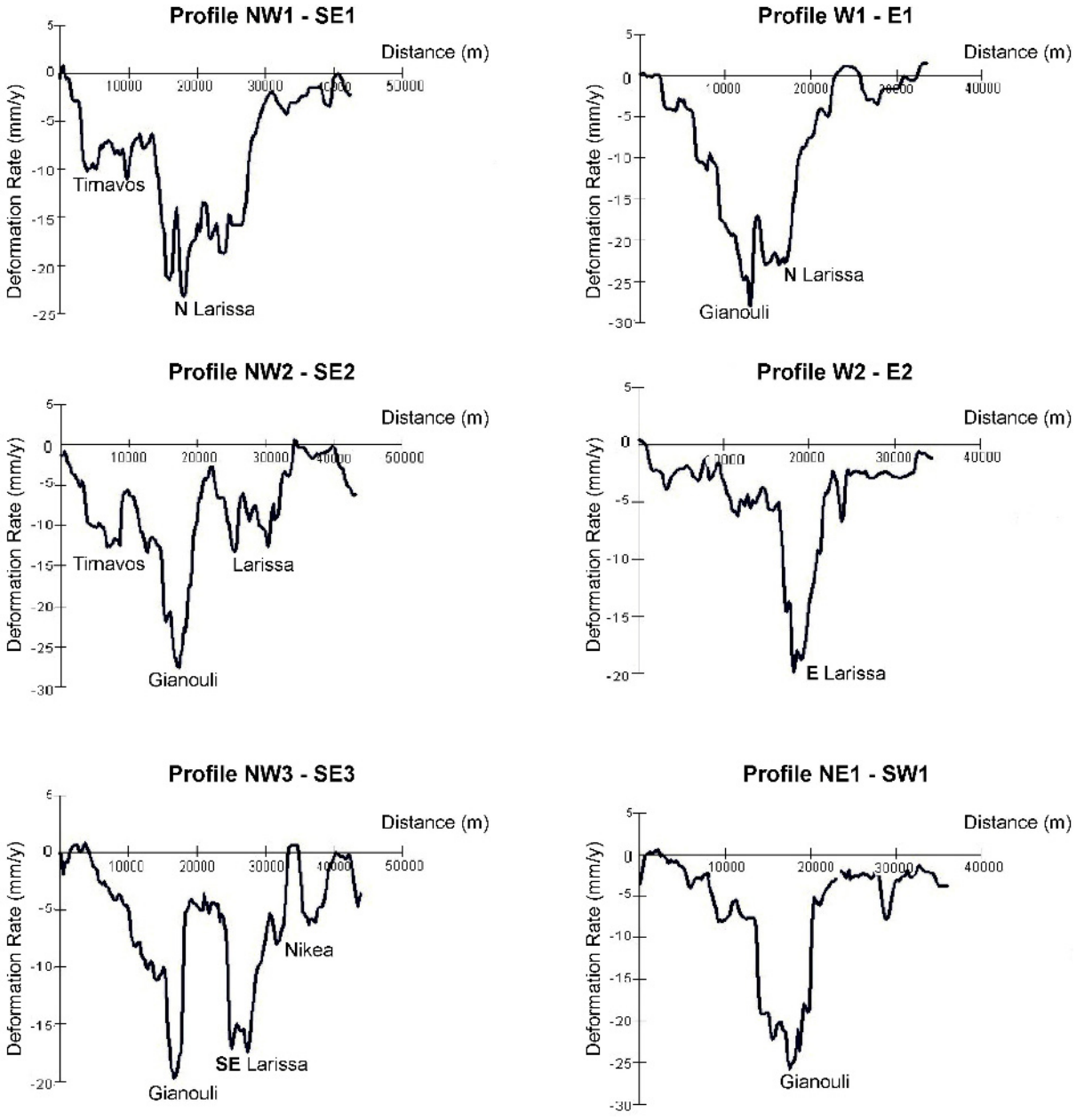

Figure 8. The variation of the deformation rate along the six profiles shown in Fig. 7 is outlined. The largest amplitude rate is measured at Gianouli and Nikea Villages.

Giannouli-Larissa Plain. The plain is characterized by low morphological slopes (0-5%) with a northern aspect of the slopes (Fig. 4). The rest of the plain regions, which are covered by alluvial, quaternary deposits and neogene lacustrine deposits seem to subside at moderate rates (about 5-10 mm/yr). The surrounding mountainous area which is covered by Alpine formations and intense morphological slopes with morphological discontinuities of the slopes have been distinguished as stable or have been slightly uplifted with respect to the NE located reference point.

Fig. 7 shows the location of the water-wells where there are data of the change in the water table level, together with some selective points of the Larissa Plain where the

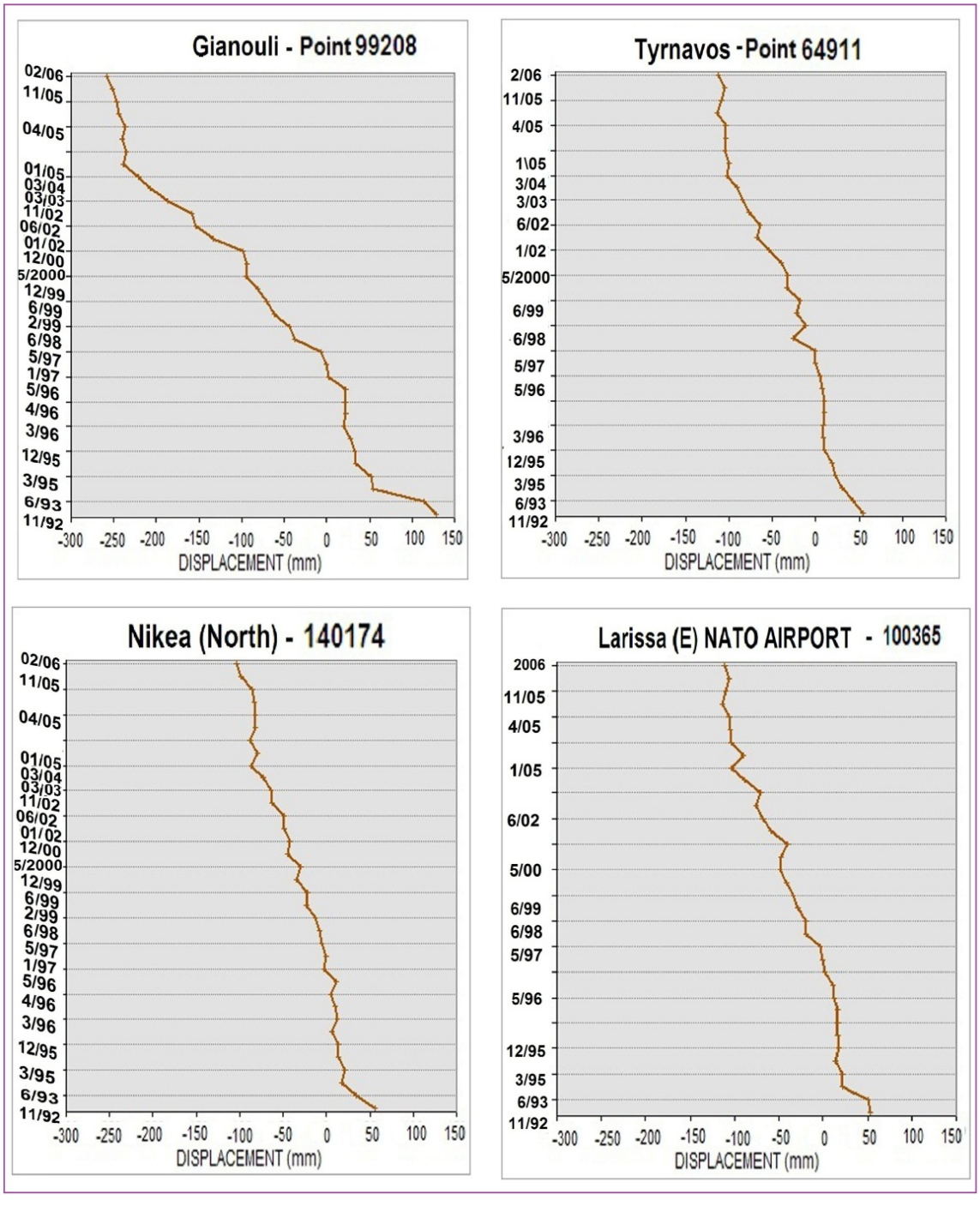

Figure 9. The displacement (in mm along the X Axis) after PSI processing in relation to the time (14 years from 1992 to 2006 along the Y Axis) for different selective points is shown in the above diagrams called "Time Series of the Deformation". The maximum subsidence takes place during spring-summer period while in the winter time the subsidence generally is decreased.

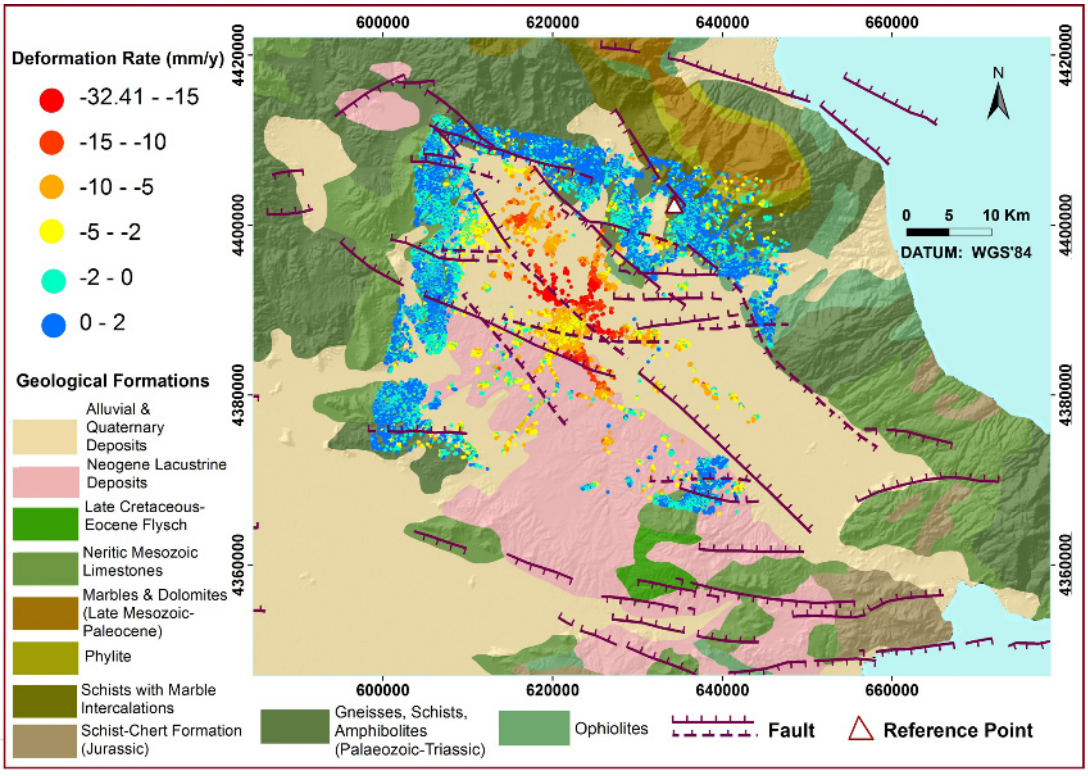

Figure 10. The geological formations and the faulting zones with the deformation rate (mm/year) based on the PSI InSAR technique of the broader area of Larissa Plain is given. Alluvial and Quaternary Deposits cover Tyrnavos-Giannouli-Larissa Plain while NW-SE and E-W faults are the boundaries of the plain. The largest amplitude rates (-25 mm/year) are observed around Larissa City, mainly along the NW-SE faulting zone which passes through.

vertical displacement is presented deduced from the PSI processing. It is evident that systematic subsidence is the predominant feature in the diagrams of the "Time Series of the Deformation", reaching maximum amplitude of about 300 mm (Gianouli area) for a time period of about 14 years. In Fig. 9 some characteristics diagrams are given. The maximum subsidence takes place during the spring-summer period while in the winter time the subsidence declines and even slight uplift can be observed. However, the Larissa City appears to be rather stable compared to its northern and eastern suburbs that are nearer to cultivated regions. It is evident that systematic subsidence is the predominant feature in these diagrams, reaching a maximum amplitude of about 300 mm (Gianouli area) for a time period of about 14 years.

Deformation rate was presented along some characteristic profiles of the Larissa Plain (Fig. 7) in order to outline the areas where the largest displacements take place. The variation of the deformation rate along these six (6) profiles is outlined in Fig. 8. The largest amplitude rate (20-30 mm/year) is observed in the northern (Gianouli area), eastern and south-eastern area of Larissa. Smaller but significant deformation rates (of about 10 mm/year) appear around the Tyrnavos Area, while in the City of Larissa, the subsidence rate is 6-10 mm/year. The deformation rate appears to be diminishing near the edges of the profiles.

As it has been mentioned previously, the observed sediment compaction in the Larissa Plain is due to the excessive water pumping for irrigation purposes, the seasonal water table variation (Fig. 11), and the declined rate in rainfall during the previous years (Fig. 12). A systematic drop of the water table is observed during 1980-2006 in all the presented wells (Fig. 7), especially to those that are located within the sedimentary basin, according to Ministry of Rural Development and Food in Athens. Two characteristic diagrams of well No 04 and 05 located within the sedimentary basin are presented in Fig. 11. It was reported by the Ministry of Rural Development and Food in Athens that the drop of the water table in the wells of the broader area of Larissa plain range between 1-11 m (with an average value of

about 4 meters) for the period 2000-2001. Note that the majority of the wells (51%) in Thessaly Plain are located within sedimentary formations, as indicated in Fig. 13.
Another factor that has to be considered is the type of cultivation (mainly large cotton fields) in the Thessaly Plain during the last 20 years which demands significantly higher quantities of water during the summer-months period (June-September). The latter correlates well with the study of selective PSI points in Larissa plain (especially in the south-eastern area, at Nikea), showing that subsidence takes place during the late spring-summer period, while uplift usually occurs during fall-winter time (Fig. 9). The type of vertical motion (uplift and subsidence) is also correlated with the monthly rain in Thessaly Plain, where low and high precipitation is observed in summer and winter months, respectively (Fig. 12). However, the subsidence rate is much higher than the uplift rate, presenting an overall subsidence during the entire observational period (1992-2006).

8. Conclusions

Strong ground subsidence in the Larissa Plain has been systematically observed throughout the period that the PSI image covers (1992-2006), as has also been reported by previous studies [23, 25–29]. The compiled GIS database offered the possibility of studying in detail the temporal vertical motion of selective points, in areas of specific interest, and to correlate the observed ground deformation with the specific geological/tectonic characteristics of the Thessaly Plain. Summarizing, the following conclusions may be outlined:

- The PSI image clearly shows that subsidence generally takes place inside the Larissa Plain ranging from 2-330 mm for the observational period (1992-2006).
- There is a correlation between the seasonal water table variation (deduced from wells data, Fig. 11), the seasonal water demand for irrigation associated with specific types of cultivation (cotton fields), the monthly rainfall (Fig. 12) and the observed subsidence rate in the rural regions of the Thessaly plain (Fig. 6, Fig. 9). The majority of the wells are located in the thick sedimentary basin where the higher subsidence rates have been observed.
- The causative effect of the significant land subsidence and the different types of the reported ground fissuring over the Thessaly Plain results from the compaction and consolidation of the loose sediments after the very intensive withdrawal of the continuously declining ground water-table, mainly for irrigation purposes.
- The local tectonic and geological conditions appear to contribute in the occurrence of land subsidence.

It is expected that the ground subsidence will continue in the Thessaly Plain, together with the fissuring in the ground, with impacts in the buildings, utility and local transportation networks. The latter is inferred by the climatological changes (annual precipitation decrease) and the constantly increase of water demand (both for urban and agricultural use).

Acknowledgements

This work was carried out within the framework of the TERRAFIRMA-1 Project [38] (http://www.terrafirma.eu.com).
Authors would like to thank Prof. E. Lagios for his comments, Marathon Data Systems for providing the ArcGIS software, Assoc. Prof. Is. Parcharidis for providing some of the hydrogeological data, as well as anonymous reviewers for their comments.

References

[1] Migiros G., Bathrellos G. D., Skilodimou H. D. and Karamousalis T., Pinios (Peneus) River (Central Greece): Hydrological-Geomorphological elements and changes during the Quaternary, *Cent. Eur. J. Geosci*, 2011, 3, 215–228, DOI: 10.2478/s13533-011-0019-1
[2] Loukas A. and Vasiliades L., Probabilistic analysis of drought spatiotemporal characteristics in Thessaly region, Greece, *Nat. Haz. Earth System Sci.*, 2004, 4, 719–731
[3] Loukas A., Mylopoulos N. A., Effects of hydro-technical projects development on water balance of Pinios river basin, Thessaly. In: PROTECTION2004: (Jun 2004).
[4] NDBHMI - National Data Bank of Hydrological & Meteorological Information, http://ndbhmi.chi.civil.ntua.gr/
[5] Dalezios N. R., Blanta A., Spyropoulos N. V., Assessment of Remotely Sensed Drought Features in Vulnerable Agriculture, *Nat. Hazards Earth Syst. Sci.*, 2012, 12, 3139–3150
[6] Pratt W. E., Johnson D. W., Local subsidence of the Goose Creek oil field, *J. Geol.*, 1926, 34, 577–590

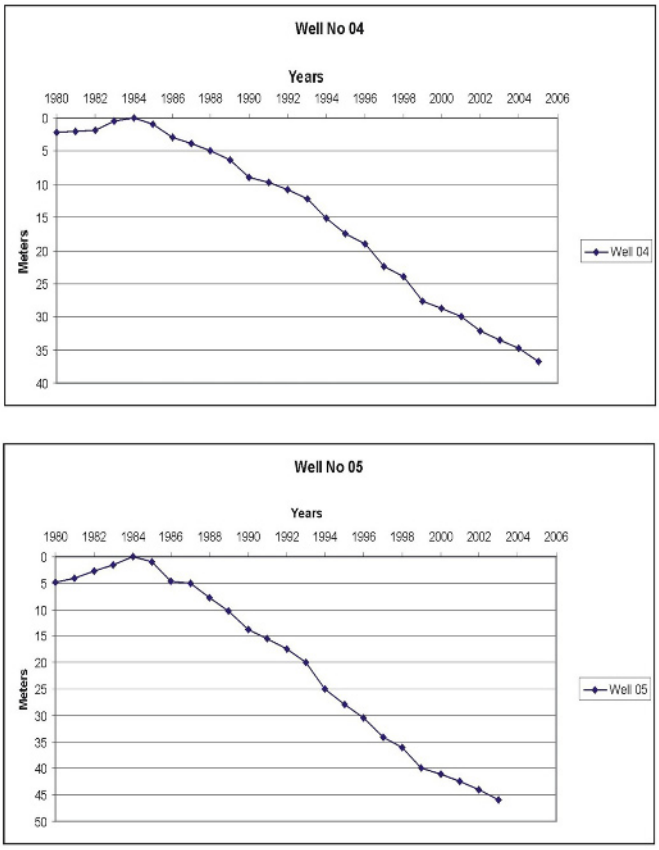

Figure 11. Change in the water table at selective wells (Ministry of Rural Development and Food). The decrease of the water table is due to the excessive water pumping for irrigation purposes during the previous years, which results in the increased sediment compaction. The wells No 04 and 05 are located within the sedimentary basin.

[7] Poland J. F., Davis G. H., Subsidence of the land surface in Tulare-Wasco and Los Banos-Kettleman City area, San Joaquin Valley California, *Trans Am Geophys Union*, 1956, 37, 287–296

[8] Chatterjee R. S., Fruneau B., Rudant J. P., Roy P. S., Frison P.-L., Lakhera R. C., Dadhwal V. K., Saha R., Subsidence of Kolkata (Calcutta) City, India during the 1990s as observed from space by Differential Synthetic Aperture Radar Interferometry (DInSAR) Technique, *Remote Sensing of Environment*, 2006, 102, 176–185

[9] Parcharidis Is., Lagios E., Sakkas V., Raucoules D., Feurer D., Le Mouelic S., King C., Carnec C., Novali F., Ferretti A., Capes R., Cooksley G., Subsidence monitoring within the Athens Basin (Greece) using space radar interferometric techniques, *Earth, Planets and Space Journal*, 2006, 58, 505–513

[10] Fruneau B., Deffontaines B., Rudant J. P., Le Parmentier A. M., Monitoring vertical deformation due to water pumping in the city of Paris (France) with differential interferometry. C. R., *Geoscience*, 2005, 337, 1173–1183

[11] Caputo R., Pavlides S., Late Cainozoic geodynamic evolution of Thessaly and surroundings (central-northern Greece), *Tectonophysics*, 1993, 223, 339–362

[12] Mountrakis D., Killias A., Pavlides S., Zouros N., Spyropoulos N., Tranos M., Soulakellis N., Field study of the Southern Thessaly highly active fault zone. Proceedings of the 2nd Congress of Greek Association of Geophysicists, Florina, 1993, 5–7

[13] Caputo R., Helly B., Pavlides S., Papadopoulos G., Palaeoseismological investigation of the Tyrnavos Fault (Thessaly, Central Greece), *Tectonophysics*, 2004, 394, 1–20

[14] Ambraseys and Jackson, Seismicity and associated strain of central Greece between 1890 and 1988,

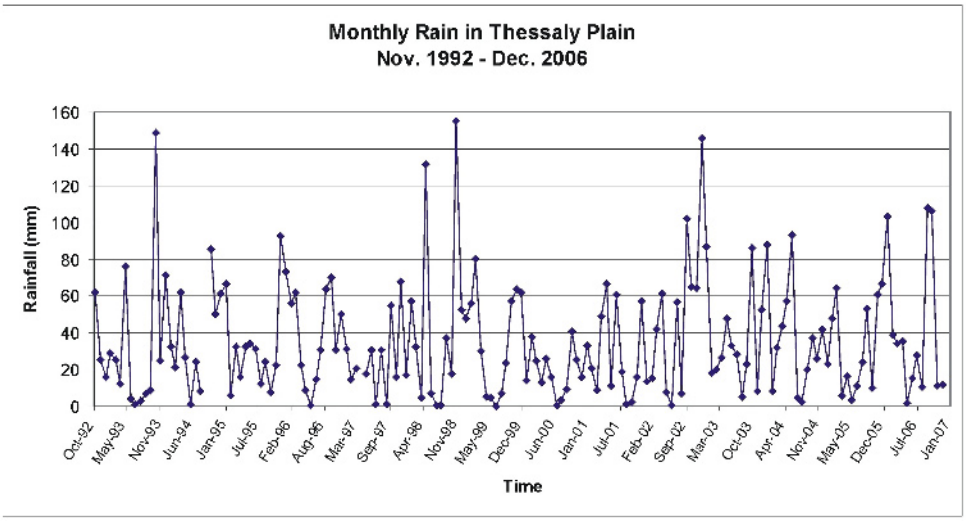

Figure 12. The vertical motions (uplift and subsidence) are also correlated with the monthly rain in Thessaly Plain, where low and high precipitation is observed in the summer and winter months, respectively (Hellenic National Meteorological Service). It is also observed that the rainfall in Thessaly Plain has been decreasing during 1992-2007.

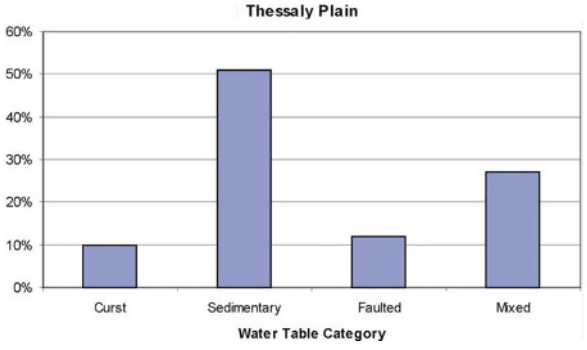

Figure 13. The majority of the wells (51%) in Thessaly plain are located within sedimentary formations (Ministry of Rural Development and Food).

Geophys J Int., 1990, 101, 663–708

[15] Papazachos B. C., Papazachou C., The earthquakes of Greece. Edition ZITI, Thessaloniki, 1997

[16] Papastamatiou D., Mouyiaris N., The earthquake of April 30, 1954, in Sophades (Central Greece), *Geophys J. R.* Astr Soc, 1986, 87, 885–895

[17] Drakos A., Stiros S., Kiratzi A., Fault-parameters of the 1980 Volos (Central Greece) earthquake (Mw = 6.5) from inversion of repeated levelling data, *Bull. Seismological Soc. Am*, 2001, 91, 1673–1684

[18] Pavlides S., Kouskouna V., Ganas A., Caputo R., Karastathis V., Sokos E., The Gonnoi (NE Thessaly - Greece) earthquake (June 2003, Ms=5.5) and the neotectonic regime of Lower Olympus. Paper presented at the 5th International Symposium on Eastern Mediterranean Geology Thessaloniki, Greece, 14-20 April, Reference T5–35, 2004

[19] Caputo R., Geological and structural study of the recent and active brittle deformation of the Neogene-Quaternary basins of Thessaly (Greece). Scientific Annals, vol. 12, Aristotle University of Thessaloniki, Thessaloniki, 1990

[20] Caputo R., Morphotectonics and kinematics along the Tirnavos Fault, northern Larissa Plain, mainland Greece, *Zeit. fur Geomorph.* 1993, 94, 167–185

[21] Caputo R., The Rodia Fault: an active complex shear zone (Larissa Basin, Central Greece), *Bull. Geol. Soc. Greece XXVII*, 1993, 447–456

[22] Athanassiou A., Neogene and Quaternary mammal faunas of Thessaly, *Annales Géologiques des Pays Helléniques*, XXXIX (A), 2002, 279–293

[23] Kontogianni V., Pytharouli Z. S., Stiros Z. S., Ground subsidence, Quaternary faults and vulnerability of utilities and transportation networks in Thessaly, Greece, *Environ. Geol.*, 2007, 52, 1085–1095

[24] Stamatis & Zagana, Hydrogeological and hydrochemical characteristics of consolidated rocks in Thessaly basin/Central Greece, *Hydrogeologie und Umwelt, Heft*, 2005, 33, 1–11

[25] Study of the Hydrogeological Conditions in Areas of the Prefecture of Larissa and Magnesias with the occurrence of Ground Fissures, Greek Institute of Geology and Mineral Exploration, 2007,

G2819/Y2047

[26] Kaplanidis A., Fountoulis D., Subsidence phenomena and ground fissures in Larissa, Karla basin, Greece: Their results in urban and rural environment. *Proc. of the Inter. Symp. "Engineering Geology and Environment"*, 1997, 1, 729–735

[27] Salvi S., Ganas A., Stramondo S., Atzori S., Tolomei C., Pepe A., Manzo M., Casu F., Berardino P., Lanari R., Monitoring Long-Term Ground Deformation by SAR Interferometry: Examples from the Abruzzi, Central Italy, and Thessaly, Greece, Paper presented at the 5th International Symposium on Eastern Mediterranean Geology, Thessaloniki, Greece, 14-20 April, 2004, Reference T7–17

[28] Ganas, Ath, ESA Announcement of Opportunity 1453: Crustal Strain Measurements in Thessaly, Central Greece by use of ERS Differential Interferometry (DInSAR). Inst. of Geodynamics, NOA & ESA. Final Report, 2006

[29] Ganas A., Salvi S., Atzori S., Tolomei C., Ground deformation in Thessaly, Central Greece, retrieved from Differential Interferometri analysis of ERS-SAR data. Abstract Volume of the 11th International Symposium on Natural and Human Induced Hazards & 2nd Workshop on Earthquake Prediction, Patras, Greece, 2006, 41

[30] Gambolati G., Gatto P., Freeze A., Mathematical simulation of the subsidence of Venice 2. Results, *Water Resources*, 1974, 10, 563–577

[31] Bell J., Helm D., Ground Cracks on Quaternary Faults in Nevada: Hydraulic and Tectonic. In: Borchers J. (ed) Land Subsidence Case Studies and Current Research: Proceedings of the Dr. Joseph F. Poland Symposium on Land Subsidence. Assoc. Eng. Geol. Special Publication 8, Star Publishing Company, 1998, 165–173

[32] Sheng Z., Helm D., Multiple Steps of Earth Fissuring caused by Ground-water withdrawal. In: Borchers J. (ed) Land Subsidence Case Studies and Current Research: Proceedings of the Dr. Joseph F. Poland Symposium on Land Subsidence, Assoc. Eng. Geol. Special Publication 8, Star Publishing Company, 1998, 149–154

[33] Gambolati G., Teatini P., Ferronato M., Anthropogenic land subsidence. In: Anderson MG (ed). Encycl Hydrol Sci. J. Wiley, 2005, 158, 2444-2459

[34] Wegmüller U., Werner C., Strozzi T., Wiesmann A., Multi-temporal interferometric point target analysis, in Analysis of Multi-temporal remote sensing images, Smits and Bruzzone (ed.), Series in Remote Sensing, 2004, 3, 136-144

[35] Wegmüller U., Werner C., Strozzi T., Wiesmann A., "ERS ASAR Integration in the Interferometric Point Target Analysis". Procs. FRINGE 2005 Workshop, Frascati, Italy, 2005 (http://earth.esa.int/workshops/fringe)

[36] Vassilopoulou S., Geodynamics of the Argolis Peninsula with GIS development and the use of Remote Sensing Data. PhD Thesis, University of Athens, Faculty of Geology, Greece, 1999 (in Greek)

[37] Vassilopoulou S., PROANA – A Useful Tool For Terrain Analysis and Geoenvironmental Applications - An Example of Studying the Geodynamic Evolution of Argolis Peninsula, Greece. Proccedings of the 20th International Cartographic Conference, Beijing, China, Chinese Society of Geodesy, Photogrammetry and Cartography, 2001, 3432–3440

[38] TERRAFIRMA - 1 Project: Pan-European Ground Motions Risk Assessment Service in Support of Policies Aimed at Protecting the Citizens against Natural & Anthropogenic Ground Motion Hazards. Global Monitoring for Environment & Security. National & Kapodistrian Univ. of Athens (NKUA), Financed by European Space Agency (ESA) & EU, 2004–2007